Journal of Science and Transport Technology
Journal homepage: https://jstt.vn/index.php/en

UNIVERSITY OF TRANSPORT TECHNOLOGY

Article info
Type of article:
Original research paper

DOI:
https://doi.org/10.58845/jstt.utt.2026.en.6.3.112-125

*Corresponding author:
Email address:
nt.khiem55@hutech.edu.vn

Received: 23/02/2026
Received in Revised Form: 06/05/2026
Accepted: 12/06/2026

Crack identification in bridge girder beam by measurements of anti-resonant frequencies

Ho Quang Quyet[1], Le Khanh Toan[1], Nguyen Thi Lan[1], Nguyen Tien Khiem[2,*]
[1]Institute of Mechanics, VAST, 264 Doi Can, Ngoc Ha Ward, Hanoi, Vietnam
[2]HUTECH University, 475A Dien Bien Phu, Thanh My Tay Ward, Ho Chi Minh City, Vietnam

Abstract: The antiresonance concept in cracked beams and its crack identification application in bridge girders represented by simply supported beams is presented in this paper. The beam model is adopted using Euler-Bernoulli beam theory, and a transversely edged crack is modelled by a rotational spring of compliance calculated from the crack depth. First, governing equations for anti-resonant frequency are established for examining anti-resonant frequencies versus locations of measuring response and excitation, as well as crack parameters. The obtained equations allow one to conduct a thorough analysis of the intricate dependence of anti-resonant frequencies on the locations where anti-resonant frequencies have been measured. It is exposed to the typical effect of a crack on anti-resonant frequencies compared to resonant ones. Finally, a crack identification approach for beams is developed using measured anti-resonant frequencies. The theoretical development is validated by experimental results and illustrated in numerical examples.

Keywords: Antiresonance, Frequency response function, Cracked beam, Structural health monitoring, Bridge girder.

1. Introduction

Resonance, a fundamental concept in structural dynamics, arises when the frequency of external excitation approaches the natural frequency of a system. When the excitation frequency lies in the vicinity of a natural frequency, the system exhibits a pronounced response characterized by a peak in vibration amplitude. Resonant frequency corresponds to the excitation frequency that produces the maximum response amplitude in forced vibration. Since resonant frequencies coincide with natural frequencies in undamped systems, they have received considerable attention in the literature on structural and mechanical vibrations. In contrast, antiresonance is characterized by an excitation frequency at which the system response amplitude becomes zero or attains its minimum value. The anti-resonant frequency corresponds to the excitation frequency at which the forced vibration response becomes zero or reaches a minimum. Obviously, antiresonance is a phenomenon inherent to multi-degree-of-freedom or distributed systems, in which anti-resonant frequencies typically occur between successive resonant frequencies. Anti-resonant frequencies have been widely utilized in vibration control [1–3] and model updating [4–7]; however, their application in structural health monitoring remains relatively unexplored [8–11]. The present study focuses on deriving governing equations for anti-resonant frequencies in cracked beams and proposing a simple approach for identifying cracks using only these frequencies.

Wang et al. [12] investigated the anti-resonant frequencies of cantilever beams systematically, and the results indicated that the anti-resonant frequency measured at the modal node coincides with the resonant frequency associated with a specific mode of vibration. The effects of cracks and excitation locations on mechanical impedances were studied by Bamnios et al. [13], and the anti-resonant frequencies for clamped and cantilever beams were extracted. The obtained results demonstrate that the mechanical impedance evaluated at the excitation point contains additional features that can be effectively utilized for detecting cracks. Simply supported Euler–Bernoulli [14] and Timoshenko [15] beams were considered in crack identification problems using this impedance method. According to Dilena and Morassi [16–19], integrating information from both resonant and anti-resonant frequencies makes it possible to identify cracks in rods and beams in many situations where approaches based solely on natural frequencies fail. Moreover, Meruane and Heylen [20] showed that combining anti-resonant and natural frequencies provides a more effective means for structural damage assessment than using mode shapes together with natural frequencies. In addition, anti-resonant frequencies are generally easier to obtain and tend to provide more reliable measurements than mode shapes. A useful procedure for crack identification was proposed by the authors of Ref. [21], using anti-resonant frequencies of multiple cracked bars, and then, an extended technique for the multi-crack detection problem in beam structures was presented in [22].

In the present study, explicit equations for anti-resonant frequencies of cracked beams are presented for the first time, enabling the analysis of their dependence on crack location, crack depth, and the response and excitation locations. Subsequently, a simplified form of the anti-resonant frequency equations is employed to identify cracks based on measurements collected at different locations. Theoretical development has been validated by experimental results and illustrated in numerical examples.

2. Anti-resonant frequency equation for cracked beams

It is well established that the frequency response function at a point x, induced by a point excitation applied at x_0 along the beam, can be determined from the corresponding governing equation.

At location x induced by a point excitation at x_0, the frequency response function (FRF) is given by the solution of

$$\frac{\partial^4 W(x,t)}{\partial x^4 EI}+\frac{\partial^2 W(x,t)}{\partial x^2 \rho F}=\delta(x-x_0)P(t), x\in(0,\ell) \quad (1)$$

subject to the following boundary conditions

$$\begin{aligned}&W^{(q_1)}(\ell,t)=W^{(p_0)}(0,t)=W^{(q_0)}(0,t)\\&=W^{(p_1)}(\ell,t)=0\end{aligned} \quad (2)$$

where the r-order derivative of $W(x,t)$ is $W^{(r)}(x,t)$ with respect to the spatial variable x, and $r=p_0$, q_0,p_1,q_1 takes values in $\{0,1,2,3\}$.

Applying the Fourier transform to Eq. (1) and (2) yield

$$\begin{aligned}&-\phi(x)\lambda^4+\phi^{(IV)}(x)=\delta(x-x_0)\bar{P}(\omega), x\in(0,1);\\&\lambda^4=\frac{\omega^2\rho F\ell^4}{EI};\bar{P}(\omega)=\frac{P(\omega)\ell^4}{EI};\end{aligned} \quad (3)$$

$$\phi^{(p_0)}(0)=\phi^{(q_0)}(0)=\phi^{(p_1)}(1)=\phi^{(q_1)}(1)=0, \quad (4)$$

where

$$P(\omega)=\int_{-\infty}^{\infty}e^{-i\omega t}P(t)dt,\ \phi(x)=\int_{-\infty}^{\infty}e^{-i\omega t}W(x,t)dt.$$

Additionally, the beam is considered to contain a crack of depth a located at e $(0\le e\le 1)$, as shown in Fig. 1. Accordingly, at the crack location, the solution of Eq. (3) is required to satisfy the following conditions

$$\begin{aligned}&\phi'''(e-0)=\phi'''(e+0),\\&\phi''(e)=\phi''(e-0)=\phi''(e+0),\\&\gamma\phi''(e)=\phi'(e+0)-\phi'(e-0),\\&\phi(e-0)=\phi(e+0).\end{aligned} \quad (5)$$

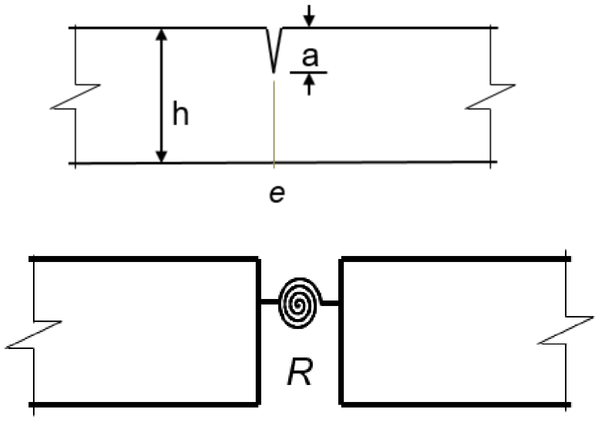

Fig. 1. Model of an edged transverse crack

The parameter γ_j, referred to as crack compliance, is determined from the crack depth as

$$\gamma = \frac{EI}{R} = \left(1-v_0^2\right)6\pi h f_c(z),$$

$$f_c(z) = z^2\begin{pmatrix} 19.6z^8 - 40.7556z^7 + 47.1063z^6 \\ -33.0351z^5 + 20.2948z^4 \\ +9.9736z^3 + 4.5948z^2 \\ -1.04533z + 0.6272 \end{pmatrix}, \quad (6)$$

$z = a/h.$

From the standpoint of differential equation theory, Eq. (3) admits a general solution that can be represented as follows

$$\phi(x) = \phi_Q(x) + \phi_0(x),$$

where $\phi_0(x,\omega)$ is the general solution of the homogeneous equation.

$$\phi^{(IV)}(x) - \lambda^4\phi(x) = 0 \quad (7)$$

and a particular solution $\phi_Q(x,\omega)$ is presented as

$$\begin{aligned}\phi_Q(x) &= \bar{P}(\omega)\int_0^x \delta(s-x_0)H(x-s)ds \\ &= H(x-x_0)\bar{P}(\omega)\end{aligned} \quad (8)$$

with

$$H(x) = \begin{cases} h(x): 0 < x \\ 0: \quad 0 \ge x \end{cases}, \quad (9)$$

$$h(x) = \left[\sinh\lambda x - \sin\lambda x\right]/2\lambda^3.$$

Alternatively, Eq. (7) admits a general solution that satisfies condition (5) along the beam span, is given by [23]

$$\phi_0(x,\omega) = C\phi_1(x,\omega) + D\phi_2(x,\omega) \quad (10)$$

where the constants C and D are determined from boundary conditions, and

$$\begin{aligned}\phi_1(x,\omega) &= L_1(x,\lambda) + \gamma L_1''(e,\lambda)K(x-e,\lambda), \\ \phi_2(x,\omega) &= L_2(x,\lambda) + \gamma L_2''(e,\lambda)K(x-e,\lambda)\end{aligned} \quad (11)$$

with

$$K(x,\lambda) = \begin{cases} 0, x \le 0 \\ S(x,\lambda), x > 0 \end{cases}, \quad (12)$$

$$S(x,\lambda) = \left[\sinh\lambda x + \sin\lambda x\right]/2\lambda.$$

In Eq. (11), the $L_1(x,\lambda)$ and $L_2(x,\lambda)$ functions represent continuous solutions of Eq. (7) satisfying the various left-end boundary conditions $x = 0$, as listed in Table 1.

As defined in Eq. (11), it is straightforward to demonstrate that the functions $L_1(x,\lambda)$ and $L_2(x,\lambda)$, satisfy the boundary conditions at the left end of the beam. Accordingly, only the boundary conditions at the right end must be imposed as

$$\begin{aligned} C\phi_1^{(p_1)}(1) + D\phi_2^{(p_1)}(1) &= -\bar{P}(\omega)h^{(p_1)}(1-x_0), \\ C\Phi_1^{(q_1)}(1) + D\Phi_2^{(q_1)}(1) &= -\bar{P}(\omega)h^{(q_1)}(\ell-x_0), \end{aligned} \quad (13)$$

where q_1 and p_1 are provided in Table 1. From Eq. (13), the constants C and D can be readily determined as follows

$$D = D_1(x_0)\bar{P}(\omega)/D(\lambda), C = C_1(x_0)\bar{P}(\omega)/D(\lambda),$$

with

$$D(\lambda) = -\phi_1^{(q_1)}(1)\phi_2^{(p_1)}(1) + \phi_1^{(p_1)}(1)\phi_2^{(q_1)}(1)$$

and

$$\begin{aligned} C_1(x_0) &= \left[h^{(q_1)}(1-x_0)\phi_2^{(p_1)}(1) - h^{(p_1)}(1-x_0)\phi_2^{(q_1)}(1)\right], \\ D_1(x_0) &= \left[h^{(p_1)}(1-x_0)\phi_1^{(q_1)}(1) - h^{(q_1)}(1-x_0)\phi_1^{(p_1)}(1)\right]. \end{aligned} \quad (14)$$

Thus, the solution of Eq. (3), fulfilling the conditions specified in (4) and (5), can be expressed in the following form

$$\begin{aligned}\phi(x,x_0,\omega) &= \left[\bar{P}(\omega)/D(\lambda)\right]\times \\ &\left[H(x-x_0)D(\lambda) + \phi_1(x)C_1(x_0) + \phi_2(x)D_1(x_0)\right]\end{aligned} \quad (15)$$

and for the damaged beam, the frequency response function can be formulated as

$$\begin{aligned} FRF(x,x_0,\omega) &= \phi(x,x_0,\omega)/\bar{P}(\omega) = \\ &\frac{[H(x-x_0)D(\lambda) + \phi_2(x)D_1(x_0) + \phi_1(x)C_1(x_0)]}{D(\lambda)}. \end{aligned} \quad (16)$$

Table 1. Derivative orders of boundary functions

Boundary conditions	Free ends	Cantilever	Simply supported ends	Clamped ends
$L_1(x,\lambda)$	$\sin\lambda x+\sinh\lambda x$	$\sinh\lambda x-\sin\lambda x$	$\sinh\lambda x$	$\sinh\lambda x-\sin\lambda x$
$L_2(x,\lambda)$	$\cos\lambda x+\cosh\lambda x$	$\cosh\lambda x-\cos\lambda x$	$\sin\lambda x$	$\cosh\lambda x-\cos\lambda x$
p_1	2	2	0	0
q_1	3	3	2	1

Resonant frequency and anti-resonant frequency, corresponding to the poles and zeros of the frequency response function, respectively, can be expressed from the corresponding frequency equations

$$D(\lambda)=\phi_1^{(p_1)}(1)\phi_2^{(q_1)}(1)-\phi_1^{(q_1)}(1)\phi_2^{(p_1)}(1)=0, \tag{17a}$$

$$\begin{gathered}A(x,x_0,\lambda)\equiv +H(x-x_0)D(\lambda)+\\ +\phi_2(x)D_1(x_0)+\phi_1(x)C_1(x_0)=0\end{gathered}. \tag{17b}$$

It should be noted that both resonant and anti-resonant frequencies obtained from Eq. (17) are governed by the parameter $\lambda=\sqrt[4]{\omega^2\rho F\ell^4/EI}$, commonly referred to as the frequency parameter. Accordingly, solving Eq. (17) with respect to λ yields the corresponding parameters of resonant and anti-resonant frequencies.

Natural or resonant frequencies are determined solely by the boundary conditions, whereas anti-resonant frequencies are significantly influenced by both the response measurement position (x) and the excitation point (x_0). In this study, these are referred to as the measurement location and the excitation location, respectively.

Substituting expressions (14) into Eq. (17b) leads to

$$\begin{gathered}A(x,x_0,\lambda)\equiv H(x-x_0)D(\lambda)\\ -A_q(x,\lambda)h^{(p_1)}(1-x_0)\\ +A_p(x,\lambda)h^{(q_1)}(1-x_0)=0,\end{gathered} \tag{18}$$

where

$$A_p(x,\lambda)=\left[\phi_2^{(p_1)}(1)\phi_1(x)-\phi_1^{(p_1)}(1)\phi_2(x)\right],$$

$$A_q(x,\lambda)=\left[\phi_2^{(q_1)}(1)\phi_1(x)-\phi_1^{(q_1)}(1)\phi_2(x)\right].$$

Note that for the resonant frequency parameter λ_k of the *k*-th mode, that means

$$D(\lambda_k)=\phi_1^{(p_1)}(1)\phi_2^{(q_1)}(1)-\phi_1^{(q_1)}(1)\phi_2^{(p_1)}(1)=0,$$

or $\phi_2^{(p_1)}(1)/\phi_1^{(p_1)}(1)=\phi_2^{(q_1)}(1)/\phi_1^{(q_1)}(1)=\mu$, therefore,

$$A_p(x,\lambda_k)=\phi_1^{(p_1)}(1)\left[\mu\phi_1(x)-\phi_2(x)\right];$$

$$A_q(x,\lambda_k)=\phi_1^{(q_1)}(1)\left[\mu\phi_1(x)-\phi_2(x)\right].$$

The latter equations imply that both $A_q(x,\lambda_k)$ and $A_p(x,\lambda_k)$ are the *k*-th mode shape of the beam, differed by a constant. Consequently, a conclusion can be made that if the frequency response function of a beam is measured at the node (zero) of a mode shape, the corresponding resonant frequency coincides with an anti-resonant frequency and is independent of crack presence. Therefore, a mode shape node is a critical position on a beam that may cause an abnormal change in anti-resonant frequency depending on the measurement location.

Furthermore, using expressions (11), the functions $D(\lambda)$, $A_q(x,\bar{\lambda}),A_p(x,\bar{\lambda})$ are rewritten by

$$\begin{gathered}D(\lambda)=D_0(\lambda)+\gamma D_1(\lambda,e)=0,\\ A_q(x,e,\lambda)=A_0^q(x,\lambda)\\ +\gamma\left[A_2^q(x,\lambda,e)L''_1(e,\lambda)-A_1^q(x,\lambda,e)L''_2(e,\lambda)\right],\\ A_p(x,e,\lambda)=A_0^p(x,\lambda)\\ +\gamma\left[A_2^p(x,\lambda,e)L''_1(e,\lambda)-A_1^p(x,\lambda,e)L''_2(e,\lambda)\right],\end{gathered} \tag{19}$$

where

$$\begin{gathered}D_0(\lambda)=L_1^{(p)}(1,\lambda)L_2^{(q)}(1,\lambda)-L_2^{(p)}(1,\lambda)L_1^{(q)}(1,\lambda),\\ D_1(\lambda,e)=S^{(p)}(1-e)\\ \times\left[-L''_2(e,\lambda)L_1^{(q)}(1,\lambda)+L_2^{(q)}(1,\lambda)L''_1(e,\lambda)\right]\\ +S^{(q)}(1-e)\\ \times\left[L''_2(e,\lambda)L_1^{(p)}(1,\lambda)-L''_1(e,\lambda)L_2^{(p)}(1,\lambda)\right];\\ A_0^{p,q}(x,\lambda)=\\ L_2^{(p,q)}(1,\lambda)L_1(x,\lambda)-L_2(x,\lambda)L_1^{(p,q)}(1,\lambda);\end{gathered} \tag{20}$$

$A_i^{p,q}(x,\lambda,e)=$
$K(x-e)L_i^{(p,q)}(1,\lambda)-L_i(x,\lambda)S^{(p,q)}(1-e),\ i=1,2$

Finally, putting (19) and (20) into (18) leads to

$$R_0(x,x_0,\lambda)+\gamma R_1(x,x_0,e,\lambda)=0, \quad (21)$$

where

$$\begin{aligned}&R_0(x,x_0,\lambda)=A_0^p(x,\lambda)h^{(q)}(1-x_0)\\&-A_0^q(x,\lambda)h^{(p)}(1-x_0)+D_0(\lambda)H(x-x_0),\\&R_1(x,x_0,e,\lambda)=A_2(x,\lambda,e)L_1''(e,\lambda)\\&-A_1(x,\lambda,e)L_2''(e,\lambda)+D_1(\lambda,e)H(x-x_0),\\&A_i(x,x_0,e,\lambda)=A_i^p(x,\lambda,e)h^{(q)}(1-x_0)\\&-A_i^q(x,\lambda,e)h^{(p)}(1-x_0),i=1,2.\end{aligned} \quad (22)$$

This equation represents the governing relation for determining anti-resonant frequencies and is derived here for the first time. It will be used in the subsequent analysis for crack identification based on anti-resonant frequencies. Obviously, the anti-resonant frequency of an intact (undamaged) beam, λ_0, can be sought from the equation

$$R_0(x,x_0,\lambda_0)=0, \quad (23)$$

solution of which is dependent upon both response measuring (x) and exciting (x_0) locations. On the other hand, the solution of the equation

$$R_1(x,x_0,e,\lambda_0)=0 \quad (24)$$

with respect to *e* gives rise to the position of the beam crack, occurred at which has no effect on the anti-resonant frequency. The crack position satisfying Eq. (24) is called crack node for a given mode of the anti-resonant frequency λ_0. Certainly, crack node also depends on the pair of driving locations (x, x_0), and this dependence is extracted from both Eq. (23) and (24) may cause difficulty in measuring anti-resonant frequencies of cracked beams. Some problems arising from the critical points would be illustrated below in numerical analysis.

3. Crack identification by anti-resonant frequencies

Consider the problem of identifying a single crack in a beam by anti-resonant frequencies measured at different pairs ($\bar{x}_k$, $\bar{x}_{0k}, k=1,\ldots,m$) of response measurement ($\bar{x}$) and excitation application ($\bar{x}_0$) locations. Suppose that anti-resonant frequencies $\bar{\omega}_1,\ldots,\bar{\omega}_m$ have been measured, and they allow one to calculate the anti-resonant frequency parameter as

$$\bar{\lambda}_k=\sqrt[4]{\bar{\omega}_k^2\rho F\ell^4/EI},k=1,\ldots,m \quad (25)$$

First, let's consider the case where two anti-resonant frequencies have been measured, so that we have $\bar{\lambda}_j$, $\bar{\lambda}_k$ given. Substituting $\bar{\lambda}_j$, $\bar{\lambda}_k$ into Eq. (21) yields

$$R_0(\bar{x}_j,\bar{x}_{0j},\bar{\lambda}_j)+\gamma R_1(\bar{x}_j,\bar{x}_{0j},e,\bar{\lambda}_j)=0,$$
$$R_0(\bar{x}_k,\bar{x}_{0k},\bar{\lambda}_k)+\gamma R_1(\bar{x}_k,\bar{x}_{0k},e,\bar{\lambda}_k)=0,$$

from which one will have

$$\begin{aligned}g_{jk}(e)&=R_0(\bar{x}_j,\bar{x}_{0j},\bar{\lambda}_j)R_1(\bar{x}_k,\bar{x}_{0k},e,\bar{\lambda}_k)\\&-R_0(\bar{x}_k,\bar{x}_{0k},\bar{\lambda}_k)R_1(\bar{x}_j,\bar{x}_{0j},e,\bar{\lambda}_j)=0.\end{aligned} \quad (26)$$

Solution of Eq. (26) with respect to e, say that is $\bar{e}_{jk}$, will give rise to the desired crack location, and therefore, crack compliance can be calculated as

$$\bar{\gamma}_{jk}=\frac{1}{2}\left[\frac{-R_0(\bar{x}_j,\bar{x}_{0j},\bar{\lambda}_j)}{R_1(\bar{x}_j,\bar{x}_{0j},\bar{e}_{jk},\bar{\lambda}_j)}+\frac{-R_0(\bar{x}_k,\bar{x}_{0k},\bar{\lambda}_k)}{R_1(\bar{x}_k,\bar{x}_{0k},\bar{e}_{jk},\bar{\lambda}_k)}\right]. \quad (27)$$

In general case, substituting the above-mentioned data $\bar{\lambda}_k, \bar{x}_k$, $\bar{x}_{0k}, k=1,\ldots,m$ into Eq. (21), one obtains equations

$$R_0(\bar{x}_k,\bar{x}_{0k},\bar{\lambda}_k)+\gamma R_1(\bar{x}_k,\bar{x}_{0k},e,\bar{\lambda}_k)=0,$$
$$k=1,2,...,m, \quad (28)$$

that are equivalent to the equation

$$g(e)=1-\frac{\left[\sum_{k=1}^m R_0(\bar{x}_j,\bar{x}_{0j},\bar{\lambda}_j)R_1(\bar{x}_j,\bar{x}_{0j},e,\bar{\lambda}_j)\right]^2}{\sum_{k=1}^m R_0^2(\bar{x}_j,\bar{x}_{0j},\bar{\lambda}_j)\sum_{k=1}^m R_1^2(\bar{x}_j,\bar{x}_{0j},e,\bar{\lambda}_j)}=0. \quad (29)$$

Obviously, the solution of the equation with respect to crack location e can be controlled by choosing various location pairs ($\bar{x}_k$, $\bar{x}_{0k}, k=1,\ldots,m$) to obtain unique solution e^*. This is typical advantage of anti-resonant frequencies in crack localization in beams in comparison with resonant frequencies. After the crack has been localized, its compliance γ can be estimated by

$$\gamma^* = -\frac{1}{m}\sum_{k=1}^{m}\left[R_0\left(\bar{x}_k, \bar{x}_{0k}, \lambda_k\right) / R_1\left(\bar{x}_k, \bar{x}_{0k}, e, \lambda_k\right)\right].$$

To complete the crack identification problem, the desired crack depth a is determined as the solution of the equation

$$6\pi\left(1-\nu_0^2\right)hf_c\left(a/h\right) = \gamma^* \quad (30)$$

with function $f_c(z)$ given above in Eq. (6), both crack location and depth have been thus identified.

4. Numerical examples and discussion

4.1. Validation of theoretical development

For validation of the theoretical development proposed above, the first anti-resonant frequency of a cracked cantilever is computed by solving Eq. (21) for various crack depths (the continuous lines in Fig. 2) and compared to the experimental one (the rectangular, triangular, circles and diamond signs) given by Bamnios et al. [13]. It can be seen very good agreement between computed and experimental results for the first anti-resonant frequency when the frequency response is calculated at positions between the crack location and the free end. The deviation increases as the response location approaches the clamped end and with increasing crack depth, but it is less than 3% only.

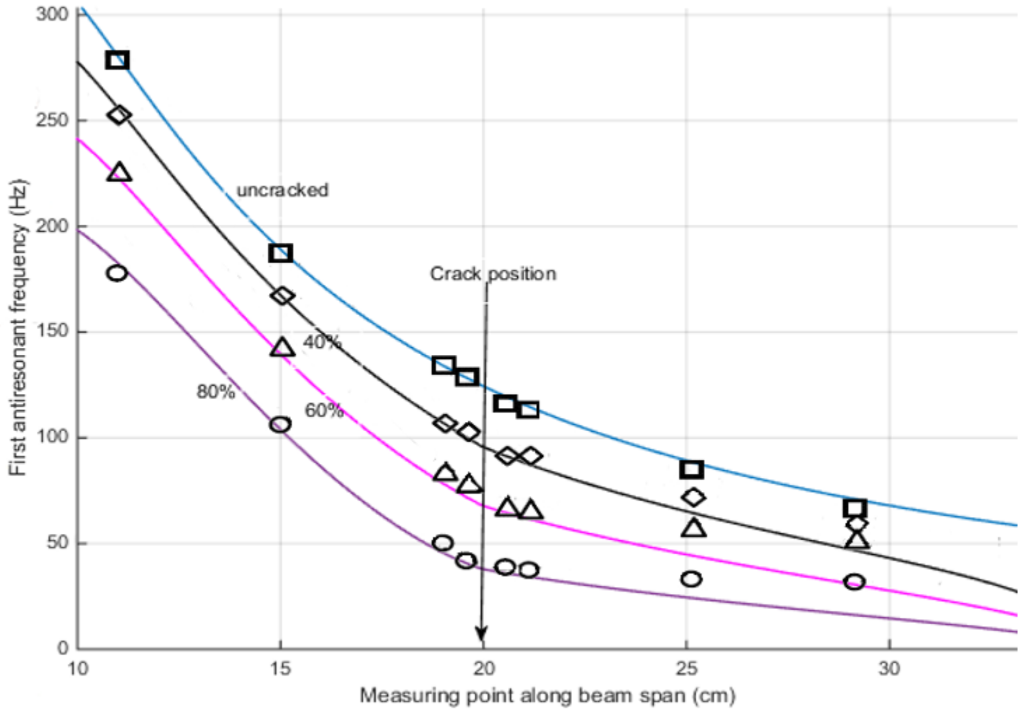

Fig. 2. Comparison of the first anti-resonant frequency calculated for the cantilever beam cracked at position (20/35) with the measured ones given in [13].

Table 2. Anti-resonant frequency (AF) parameters of intact simply supported beams in dependence upon FRF measurement locations (locations of response measurements and excitation application)

Response locations	Excitation locations						
	0.15	0.28	0.40	0.50	0.60	0.72	0.85
0.15	4.4092	4.7991	5.4173	6.2832	3.1416	3.1416	3.1416
0.28	4.7991	5.0179	5.5205	6.2832	3.1416	3.1416	3.1416
0.40	5.4173	5.5205	5.7826	6.2832	3.1416	3.1416	3.1416
0.50	6.2832	6.2832	6.2832	6.2832	6.2832	6.2832	6.2832
0.60	3.1416	3.1416	3.1416	6.2832	5.7826	5.5205	5.4173
0.72	3.1416	3.1416	3.1416	6.2832	5.5205	5.0179	4.7991
0.85	3.1416	3.1416	3.1416	6.2832	5.4173	4.7991	4.4092

First and second resonant frequency parameters of intact simply supported beams: 3.1416, 6.2832

Table 3. Anti-resonant frequency (AF) parameters of cracked SS-beams versus crack locations with crack depth a/h = 30%

Response locations	Excitation locations							Crack location
	0.15	0.28	0.40	0.50	0.60	0.72	0.85	
0.15	4.4092	4.7991	5.4173	6.2832	3.1416	3.1416	3.1416	Intact
	4.3881	4.7847	5.4057	6.2561	3.1348	3.1348	3.1348	0.25
	4.4284	4.8017	5.4131	6.2739	3.1293	3.1293	3.1293	0.40
	4.4732	4.8239	5.4278	6.2832	3.1280	3.1280	3.1280	0.50
	4.5337	4.8562	5.4550	6.2739	3.1293	3.1293	3.1293	0.60
	4.6530	4.9217	5.5247	3.1348	3.1348	3.1348	3.1348	0.75
0.28	4.7991	5.0179	5.5205	6.2832	3.1416	3.1416	3.1416	Intact
	4.7598	4.9991	5.5070	6.2561	3.1348	3.1348	3.1348	0.25
	4.7984	5.0137	5.5134	6.2739	3.1293	3.1293	3.1293	0.40
	4.8625	5.0393	5.5284	6.2832	3.1280	3.1280	3.1280	0.50
	4.9562	5.0758	5.5539	6.2739	3.1293	3.1293	3.1293	0.60
	5.2085	5.1557	5.6209	3.1348	3.1348	3.1348	3.1348	0.75
0.40	5.4173	5.5205	5.7826	6.2832	3.1416	3.1416	3.1416	Intact
	5.3936	5.5070	5.7708	6.2561	3.1348	3.1348	3.1348	0.25
	5.3579	5.4946	5.7674	6.2739	3.1293	3.1293	3.1293	0.40
	5.4388	5.5269	5.7843	6.2832	3.1280	3.1280	3.1280	0.50
	5.5554	5.5646	5.8036	6.2739	3.1293	3.1293	3.1293	0.60
	5.9215	5.6587	5.8573	6.2561	3.1348	3.1348	3.1348	0.75
0.50	6.2832	6.2832	6.2832	6.2832	6.2832	6.2832	6.2832	Intact
	6.2561	6.2561	6.2561	6.2559	6.2447	6.2389	6.2369	0.25
	6.2739	6.2739	6.2739	6.2739	6.2734	6.2731	6.2730	0.40
	6.2832	6.2832	6.2832	6.2832	6.2832	6.2832	6.2832	0.50
	6.2731	6.2731	6.2734	6.2739	6.2739	6.2739	6.2739	0.60
	6.2522	6.2453	6.2482	6.2561	6.2561	6.2561	6.2561	0.75
0.60	3.1416	3.1416	3.1416	6.2832	5.7826	5.5205	5.4173	Intact
	3.1348	3.1348	3.1348	6.2447	5.7491	5.4892	5.3865	0.25
	3.1293	3.1293	3.1293	6.2734	5.7676	5.5029	5.3985	0.40
	3.1280	3.1280	3.1280	6.2832	5.7825	5.5192	5.4154	0.50
	3.1293	3.1293	3.1293	6.2530	5.7674	5.5134	5.4131	0.60
	3.1348	3.1348	3.1348	6.1829	5.7482	5.5040	5.4057	0.75
0.72	3.1416	3.1416	3.1416	6.2832	5.5205	5.0179	4.7991	Intact
	3.1348	3.1348	3.1348	6.2389	5.4892	4.9943	4.7781	0.25
	3.1293	3.1293	3.1293	6.2731	5.5029	4.9990	4.7799	0.40
	3.1280	3.1280	3.1280	6.2832	5.5192	5.0124	4.7915	0.50
	3.1293	3.1293	3.1293	6.2436	5.5134	5.0176	4.7991	0.60
	3.1348	3.1348	3.1348	6.1342	5.4584	4.9926	4.7847	0.75
0.85	3.1416	3.1416	3.1416	6.2832	5.4173	4.7991	4.4092	Intact
	3.1348	3.1348	3.1348	6.2369	5.3865	4.7781	4.3932	0.25
	3.1293	3.1293	3.1293	6.2730	5.3985	4.7799	4.3914	0.40
	3.1280	3.1280	3.1280	6.2832	5.4154	4.7915	4.3990	0.50
	3.1293	3.1293	3.1293	6.2404	5.4131	4.7991	4.4074	0.60
	3.1348	3.1348	3.1348	6.1192	5.3530	4.7788	4.4031	0.75

First and second resonant frequency parameters: 3.1416, 6.2832 (a/h =0) and a/h = 0.3: 3.1347, 6.2561 (e=0.25); 3.1292, 6.2738 (e= 0.4); 3.1279, 6.2832 (e = 0.5); 3.1292, 6.2738(e = 0.6); 3.1347, 6.2561 (e = 0.75)

Table 4. Anti-resonant frequency (AF) parameters of SS-beam cracked at symmetric locations (e/L = 0.25 & 0.75)

Res-ponse location	Excitation locations										Crack depth
	0.15		0.28		0.5		0.72		0.85		
	e=0.25	e=0.75	e=0.25	e=0.75	e=0.25	e=0.75	e=0.25	e=0.75	e=0.25	e=0.75	
0.15	4.4092	4.4092	4.7991	4.7991	6.2832	6.2832	3.1416	3.1416	3.1416	3.1416	0%
	4.4067	4.4317	4.7975	4.8117	6.2802	6.2802	3.1409	3.1409	3.1409	3.1409	10%
	4.3999	4.5018	4.7929	4.8491	6.2715	6.2715	3.1387	3.1387	3.1387	3.1387	20%
	4.3881	4.6530	4.7847	4.9217	6.2561	3.1348	3.1348	3.1348	3.1348	3.1348	30%
	4.3698	5.1400	4.7717	5.0630	6.2310	3.1282	3.1282	3.1282	3.1282	3.1282	40%
0.28	4.7991	4.7991	5.0179	5.0179	6.2832	6.2832	3.1416	3.1416	3.1416	3.1416	0%
	4.7946	4.8332	5.0158	5.0320	6.2802	6.2802	3.1409	3.1409	3.1409	3.1409	10%
	4.7818	4.9426	5.0098	5.0741	6.2715	6.2715	3.1387	3.1387	3.1387	3.1387	20%
	4.7598	5.2085	4.9991	5.1557	6.2561	3.1348	3.1348	3.1348	3.1348	3.1348	30%
	4.7259	3.1282	4.9821	5.3153	6.2310	3.1282	3.1282	3.1282	3.1282	3.1282	40%
0.5	6.2832	6.2832	6.2832	6.2832	6.2832	6.2832	6.2832	6.2832	6.2832	6.2832	0%
	6.2802	6.2783	6.2802	6.2784	6.2802	6.2802	6.2783	6.2802	6.2780	6.2802	10%
	6.2715	6.2667	6.2715	6.2654	6.2715	6.2715	6.2640	6.2715	6.2632	6.2715	20%
	6.2561	6.2522	6.2561	6.2453	6.2559	6.2561	6.2389	6.2561	6.2369	6.2561	30%
	6.2310	6.2310	6.2310	6.2186	6.2302	6.2310	6.1982	6.2310	6.1944	6.2310	40%
0.72	3.1416	3.1416	3.1416	3.1416	6.2832	6.2832	5.0179	5.0179	4.7991	4.7991	0%
	3.1409	3.1409	3.1409	3.1409	6.2783	6.2652	5.0153	5.0151	4.7968	4.7975	10%
	3.1387	3.1387	3.1387	3.1387	6.2635	6.2179	5.0078	5.0069	4.7901	4.7929	20%
	3.1348	3.1348	3.1348	3.1348	6.2377	6.1225	4.9943	4.9926	4.7781	4.7847	30%
	3.1282	5.6238	3.1282	3.1282	6.1959	5.9795	4.9723	4.6789	4.7585	4.7717	40%
0.85	3.1416	3.1416	3.1416	3.1416	6.2832	6.2832	4.7991	4.7991	4.4092	4.4092	0%
	3.1409	3.1409	3.1409	3.1409	6.2780	6.2646	4.7968	4.7968	4.4074	4.4085	10%
	3.1387	3.1387	3.1387	3.1387	6.2632	6.2114	4.7901	4.7903	4.4023	4.4065	20%
	3.1348	3.1348	3.1348	3.1348	6.2369	6.1192	4.7781	4.7788	4.3932	4.4031	30%
	3.1282	5.6950	3.1282	3.1282	6.1944	5.9768	4.7585	4.7606	4.3782	4.3976	40%

First and second resonant frequency parameters equal 3.1416, 6.2832 (a/h = 0) and 3.1408, 6.2802 (a/h = 0.1); 3.1387, 6.2715 (a/h = 0.2); 3.1347, 6.2561(a/h= 0.3); 3.1282, 6.2310 (a/h = 0.4) when ec = 0.25 and 3.1408, 6.2802 (a/h = 0.1);3.1387, 6.2715 (a/h = 0.2); 3.1347, 6.2561(a/h= 0.3); 3.1282, 6.2310 (a/h=0.4) when e = 0.75

4.2. Effect of frequency response function (FRF) measurement locations

First, let's consider the anti-resonant frequency of undamaged simply supported beam in dependence on the locations where the frequency response function has been measured. Numerical results obtained as solution of Eq. (23) for anti-resonant frequency parameters are shown in Table 2, where the locations used for response measurements and excitation application are running through 0.15, 0.28, 0.4, 0.5, 0.6, 0.72, and 0.85. These locations are chosen for testing the symmetry of FRF and examining the above-mentioned overlap of resonant and anti-resonant frequency when FRF is measured at the beam middle 0.5, which is the node of the second mode shape.

Clearly, the anti-resonant frequency of intact beam is unchanged under interchange of locations where response is measured and excitation is applied. This is obviously because of the well-known reciprocity theorem applied for the frequency response function, $\mathrm{FRF}(x, x_0, \omega) = \mathrm{FRF}(x_0, x, \omega)$. Also, anti-resonant frequencies of beams with symmetric boundary conditions, such as simply supported beams, measured at symmetric pairs of response and excitation locations are the same, for instance, 5.5205 measured at location pairs (0.28, 0.40) and (0.72, 0.60) or 5.0179 measured at (0.28, 0.28) and (0.72, 0.72), etc. On the other hand, it is observed that for both cases when response is measured or excitation is applied at the beam middle (0.5), the anti-resonant frequency is identical to the second resonant frequency (6.2832) since the beam middle is node of the second mode shape of simply supported beam. Finally, it is worth noting that for response measured or excitation applied at locations after the critical point ($x > 0.5, x_0 < 0.5$ or $x \langle 0.5, x_0 \rangle 0.5$), the anti-resonant frequency returns to the first resonant frequency. This means that in the case of no anti-resonant frequency existing between the first and second resonant frequencies. Therefore, it can be concluded that anti-resonant frequencies could be found truthfully for the response measurement and excitation application locations, both chosen on the left ($x < 0.5, x_0 < 0.5$) or on the right ($x > 0.5, x_0 > 0.5$) of the beam middle (0.5). Otherwise, the anti-resonant frequency would be found as either the first or second resonant frequencies; they are both critical anti-resonant frequencies. Nevertheless, anti-resonant frequency can be confidently calculated for every location in beam overlapped with both response measurement and excitation application locations.

4.3. Effect of cracks on anti-resonant frequency

Anti-resonant frequency of cracked simply supported beam calculated as the minimum of FRF in the frequency segment between the first and second resonant frequencies of the beam is demonstrated in Tables 3 – 5. Namely, Table 3 shows anti-resonant frequency calculated for various pairs of response-excitation locations (REL) in different locations (e/L=0.25, 0.40, 0.50, 0.60, 0.75) of the crack with depth 30%. Results presented in the Table ensure again that the anti-resonant frequency of the cracked beam could be consistently determined for REL chosen in the intervals: I_1 = (0.0 – 0.5) and I_2 = (0.5 – 1.0) as mentioned above for intact beam. The anti-resonant frequencies determined outside the intervals are all critical (equal to resonant ones). Obviously, crack may increase the anti-resonant frequencies determined in I_1, but it can only reduce the anti-resonant frequency measured in I_2. Moreover, as shown in Table 4, cracks abolish the reciprocity theorem in calculating anti-resonant frequencies by FRF, and symmetric cracks in beam with symmetrical boundary conditions affect unequally on anti-resonant frequency that is, unlike the effect of such cracks on resonant frequencies. Observing data given in Table 5 we can see that anti-resonant frequency measured at the midspan of either intact or cracked beams is consistently equal to the second resonant frequency. This is because midspan is node of second mode shape, as mentioned above, being a critical point for anti-resonant frequencies. Also, anti-resonant frequencies measured at locations after the critical point remain equal to the first resonant frequencies, though they are modified by crack presence. Finally, it is worth noting that anti-resonant frequencies may increase due to crack presence, depending on where they are measured, while resonant frequencies could only be reduced due to the crack. This is one of the typical features for anti-resonant frequencies of cracked beam compared to the resonant ones.

4.4. Crack identification results

The crack detection procedure proposed in section 3 is tested for a simply supported beam in two crack scenarios I and II with crack locations e/L = 0.25 and 0.75 respectively. In both the scenarios, crack depth is of 10% beam thickness.

The procedure is first checked for crack localization by examining the diagnosis function $g_{jk}(e)$ defined in Eq. (29) with different scenarios of response-excitation locations given in the first column of Table 5. Namely, the diagnosis function is calculated first for various crack depths and then for different selections of response-excitation locations, and the results are presented in Fig. 3 for the crack scenario I and Fig. 4 for scenario II. Obviously, in both cases of tested scenarios, the unique crack location is exactly detected at 0.25 and 0.75 (the second zero crossing point of the curves is a false crack location because it varies with response-excitation locations). Crack depth estimated by solving Eq. (26) and (27) are provided in Table 6. Visibly, the estimated crack depth has a small error of about 1%.

Table 5. Anti-resonant frequency (AF) parameters of cracked at midspan (e/L = 0.5) of SS-beams

Response locations	Excitation locations							Crack depth
	0.15	0.28	0.40	0.50	0.60	0.72	0.85	
	4.4092	4.7991	5.4173	6.2832	3.1416	3.1416	3.1416	0%
	4.4163	4.8019	5.4185	6.2832	3.1401	3.1401	3.1401	10%
0.15	4.4368	4.8098	5.4219	6.2832	3.1358	3.1358	3.1358	20 %
	4.4732	4.8239	5.4278	6.2832	3.1280	3.1280	3.1280	30 %
	4.5322	4.8467	5.4374	6.2832	3.1152	3.1152	3.1152	40 %
	4.7991	5.0179	5.5205	6.2832	3.1416	3.1416	3.1416	0%
	4.8063	5.0204	5.5214	6.2832	3.1401	3.1401	3.1401	10%
0.28	4.8268	5.0272	5.5239	6.2832	3.1358	3.1358	3.1358	20 %
	4.8625	5.0393	5.5284	6.2832	3.1280	3.1280	3.1280	30 %
	4.9190	5.0588	5.5357	6.2832	3.1152	3.1152	3.1152	40 %
	5.4173	5.5205	5.7826	6.2832	3.1416	3.1416	3.1416	0 %
	5.4198	5.5212	5.7828	6.2832	3.1401	3.1401	3.1401	10 %
0.40	5.4268	5.5233	5.7834	6.2832	3.1358	3.1358	3.1358	20 %
	5.4388	5.5269	5.7843	6.2832	3.1280	3.1280	3.1280	30 %
	5.4573	5.5327	5.7859	6.2832	3.1152	3.1152	3.1152	40 %
	6.2832	6.2832	6.2832	6.2832	6.2832	6.2832	6.2832	0%
	6.2832	6.2832	6.2832	6.2832	6.2832	6.2832	6.2832	10 %
0.50	6.2832	6.2832	6.2832	6.2832	6.2832	6.2832	6.2832	20 %
	6.2832	6.2832	6.2832	6.2832	6.2832	6.2832	6.2832	30 %
	6.2832	6.2832	6.2832	6.2832	6.2832	6.2832	6.2832	40 %
	3.1416	3.1416	3.1416	6.2832	5.7826	5.5205	5.4173	0 %
	3.1401	3.1401	3.1401	6.2832	5.7826	5.5204	5.4171	10 %
0.60	3.1358	3.1358	3.1358	6.2832	5.7826	5.5199	5.4165	20 %
	3.1280	3.1280	3.1280	6.2832	5.7825	5.5192	5.4154	30 %
	3.1152	3.1152	3.1152	6.2832	5.7823	5.5181	5.4135	40 %
	3.1416	3.1416	3.1416	6.2832	5.5205	5.0179	4.7991	0 %
	3.1401	3.1401	3.1401	6.2832	5.5204	5.0173	4.7983	10 %
0.72	3.1358	3.1358	3.1358	6.2832	5.5199	5.0155	4.7959	20 %
	3.1280	3.1280	3.1280	6.2832	5.5192	5.0124	4.7915	30 %
	3.1152	3.1152	3.1152	6.2832	5.5181	5.0072	4.7844	40 %
	3.1416	3.1416	3.1416	6.2832	5.4173	4.7991	4.4092	0 %
	3.1401	3.1401	3.1401	6.2832	5.4171	4.7983	4.4080	10 %
0.85	3.1358	3.1358	3.1358	6.2832	5.4165	4.7959	4.4048	20 %
	3.1280	3.1280	3.1280	6.2832	5.4154	4.7915	4.3990	30 %
	3.1152	3.1152	3.1152	6.2832	5.4135	4.7844	4.3895	40 %

First and second resonant frequency parameters: 3.1416, 6.2832 (a/h =0) and 3.1401, 6.2832 (a/h= 0.1); 3.1357, 6.2832 (a/h= 0.2); 3.1279, 6.2832 (a/h= 0.3); 3.1151, 6.2832 (a/h=0.4) when e = 0.5

5. Concluding remarks

Thus, a zero of the frequency response function, referred to as the anti-resonant frequency, is adopted for crack identification in bridge girder beams. First, the so-called anti-resonant frequency equation (AFE) is conducted for a beam with a single crack represented by a rotational spring model. The established AFE shows immediately the fact that anti-resonant frequencies of a beam structure are strongly dependent on both the locations where the response is measured and the exciting force is applied. This is contrary to resonant frequencies that are independent of the driving locations. This local feature of anti-resonant frequencies makes them have more interesting properties needed to be specifically investigated.

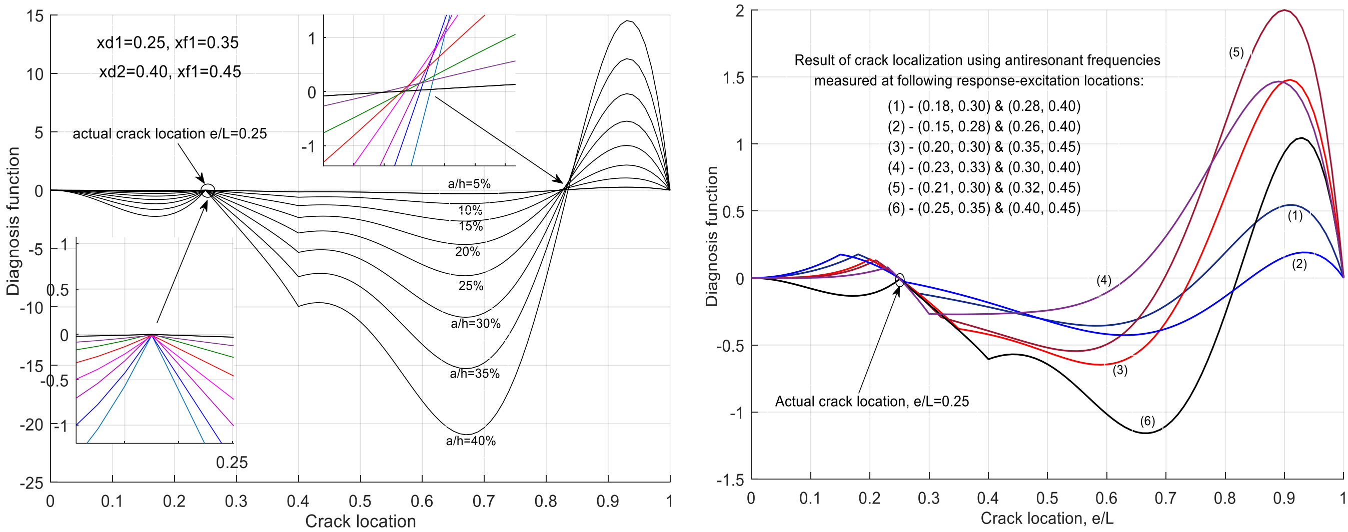

Fig. 3. Results of crack localization using anti-resonant frequencies measured at different pairs of response-excitation locations. Actual crack location e/L = 0.25 (a/h=10%).

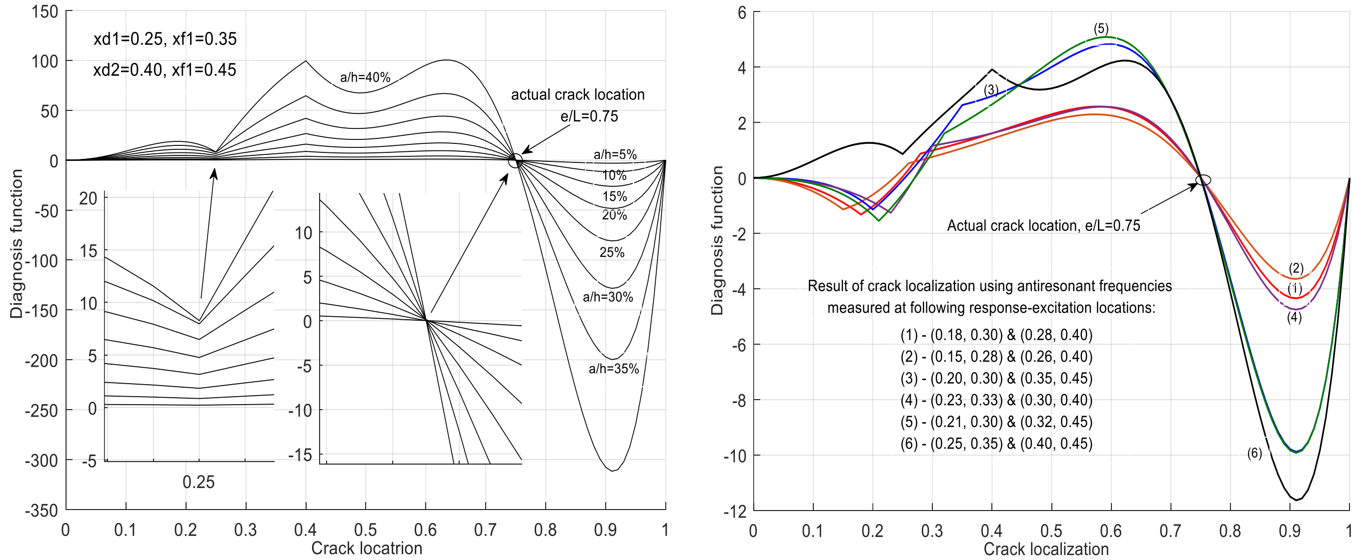

Fig. 4. Results of crack localization using anti-resonant frequencies measured at different pairs of response-excitation locations. Actual crack location e/L = 0.75 (a/h=10%).

Second, using the AFE, anti-resonant frequencies of the cracked beam are thoroughly examined along both the response-excitation locations and crack parameters, such as its location and depth. Analysis of anti-resonant frequencies in dependence upon response-excitation locations exposed that anti-resonant frequencies measured at some specific locations are identical to resonant ones. Otherwise speaking, an actual anti-resonant frequency cannot be measured at arbitrarily chosen response-excitation locations. Therefore, attention should be paid to selecting response-excitation locations for obtaining the desired anti-resonant frequency. Also, analysis of crack-dependent anti-resonant frequencies shows an interesting fact that a crack may not only abolish the reciprocity theorem applied for intact FRF but also increase anti-resonant frequencies measured at specific locations. This is a typical distinction of anti-resonant frequencies of a cracked beam in comparison with resonant ones, which can only be reduced due to crack presence. Finally, the dependence of anti-resonant frequencies on response-excitation locations enables propose a simple procedure for crack detection in a beam using anti-resonant frequencies alone. The proposed procedure allows for easily getting a unique solution in crack localization in beams with symmetric boundary conditions that cannot be obtained if only resonant frequencies are employed.

Table 6. Results of crack identification by anti-resonant frequencies along the various scenarios of response measurement and excitation locations

Scenarios for Response - excitation locations	Crack scenario I		Crack scenario II	
	Detected crack location	Estimated crack depth	Detected crack location	Estimated crack depth
(1): (0.18-0.28) & (0.3- 0.4)	0.25	9.89 %	0.75	10.02 %
(2): (0.15-0.28) & (0.26 - 0.4)	0.25	9.92 %	0.75	10.01 %
(3): (0.2 - 0.3) & (0.35- 0.45)	0.25	9.89 %	0.75	10.01 %
(4): (0.23 - 0.33) & (0.3- 0.4)	0.25	9.98 %	0.75	10.02 %
(5): (0.21- 0.3) & (0.32- 0.45)	0.25	9.93 %	0.75	10.02 %
(6): (0.25 - 0.35) & (0.4 - 0.45)	0.25	9.90 %	0.75	10.02 %
Actual crack scenarios	e/L = 0.25	a/h = 10%	e/L= 0.75	a/h = 10%

The proposed approach in this study has been validated by experimental results published earlier and illustrated by numerical examples.

Acknowledgement

This study was completed with support from Institute of Mechanics, VAST under a project of number CSCL03.03/25-26.

Declaration of Generative AI

During the preparation of this work, the authors do not use Generative AI and AI-assisted technologies tools in order to generate the content of the manuscript.

References

[1]. J.E. Mottershead, Y.M. Ram. (2006). Inverse eigenvalue problems in vibration absorption: Passive modification and active control. *Mechanical Systems and Signal Processing*, 20(1), 5–44. https://doi.org/10.1016/j.ymssp.2005.05.006

[2]. J.E. Mottershead, M.G. Tehrani, S. James, Y.M. Ram. (2008). Active vibration suppression by pole-zero placement using measured receptances. *Journal of Sound and Vibration*, 311(3–5), 1391–1408. https://doi.org/10.1016/j.jsv.2007.10.024

[3]. D. Richiedei, I. Tamellin. (2021). Active control of linear vibrating systems for antiresonance assignment with regional pole placement. *Journal of Sound and Vibration*, 494, Article 115858. https://doi.org/10.1016/j.jsv.2020.115858

[4]. J.E. Mottershead. (1998). On the zeros of structural frequency response functions and their sensitivities. *Mechanical Systems and Signal Processing*, 12(5), 591–597. https://doi.org/10.1006/mssp.1998.0167

[5]. W. D'Ambrogio, A. Fregolent. (2000). The use of antiresonances for robust model updating. *Journal of Sound and Vibration*, 236(2), 227–243. https://doi.org/10.1006/jsvi.1999.2987

[6]. K. Jones, J. Turcotte. (2002). Finite element model updating using antiresonant frequencies. *Journal of Sound and Vibration*, 252(4), 717–727. https://doi.org/10.1006/jsvi.2001.3697

[7]. V. Meruane. (2013). Model updating using antiresonant frequencies identified from transmissibility functions. *Journal of Sound and Vibration*, 332(4), 807–820. https://doi.org/10.1016/j.jsv.2012.10.021

[8]. F. Wahl, G. Schmidt, L. Forrai. (1999). On the significance of antiresonance frequencies in experimental structural analysis. *Journal of Sound and Vibration*, 219(3), 379–394. https://doi.org/10.1006/jsvi.1998.1831

[9]. D. Hanson, T.P. Waters, D.J. Thompson, R.B. Randall, R.A.J. Ford. (2007). The role of anti-resonance frequencies from operational modal analysis in finite element model updating. *Mechanical Systems and Signal Processing*, 21(1), 74–97. https://doi.org/10.1016/j.ymssp.2006.01.001

[10]. T. Inada, Y. Shimamura, A. Todoroki, H. Kobayashi. (2004). Development of the Two-Step Delamination Identification Method by Resonant and Anti-Resonant Frequency Changes. *Key Engineering Materials*, 270–273, 1852–1858. https://doi.org/10.4028/www.scientific.net/KEM.270-273.1852

[11]. N. Dharmaraju, J.K. Sinha. (2005). Some comments on use of antiresonance for crack identification in beams. *Journal of Sound and Vibration*, 286(3), 669–671. https://doi.org/10.1016/j.jsv.2005.01.001

[12]. W. Feng-Quan, H. Xiao-Ling, G. Ying-Zheng. (1996). Analysis of the Characteristics of Pseudo-Resonance and Anti-Resonance. *Journal of Vibration and Acoustics*, 118(4), 663–667. https://doi.org/10.1115/1.2888349

[13]. Y. Bamnios, E. Douka, A. Trochidis. (2002). Crack identification in beam structures using mechanical impedance. *Journal of Sound and Vibration*, 256(2), 287–297. https://doi.org/10.1006/jsvi.2001.4209

[14]. D.S. Wang, H.P. Zhu. (2005). Wave Propagation Based Multi-Crack Identification in Beam Structures through Anti-Resonances Information. *Key Engineering Materials*, 293–294, 557–564. https://doi.org/10.4028/0-87849-976-8.557

[15]. D. Wang, H. Zhu, C. Chen, Y. Xia. (2007). An impedance analysis for crack detection in the Timoshenko beam based on the anti-resonance technique. *Acta Mechanica Solida Sinica*, 20(3), 228–235. https://doi.org/10.1007/s10338-007-0727-8

[16]. M. Dilena, A. Morassi. (2003). Detecting cracks in a longitudinally vibrating beam with dissipative boundary conditions. *Journal of Sound and Vibration*, 267(1), 87–103. https://doi.org/10.1016/S0022-460X(03)00176-7

[17]. M. Dilena, A. Morassi. (2004). The use of antiresonances for crack detection in beams. *Journal of Sound and Vibration*, 276(1–2), 195–214. https://doi.org/10.1016/j.jsv.2003.07.021

[18]. M. Dilena, A. Morassi. (2009). Structural Health Monitoring of Rods Based on Natural Frequency and Antiresonant Frequency Measurements. *Structural Health Monitoring*, 8(2), 149–173. https://doi.org/10.1177/1475921708102103

[19]. M. Dilena, A. Morassi. (2010). Reconstruction Method for Damage Detection in Beams Based on Natural Frequency and Antiresonant Frequency Measurements. *Journal of Engineering Mechanics*, 136(3), 329–344. https://doi.org/10.1061/(ASCE)0733-9399(2010)136:3(329)

[20]. V. Meruane, W. Heylen. (2011). Structural damage assessment with antiresonances versus mode shapes using parallel genetic algorithms. *Structural Control and Health Monitoring*, 18(8), 825–839. https://doi.org/10.1002/stc.401

[21]. T.T. Hai, K. Nguyen, P.T.B. Lien. (2019). Characteristic equation for antiresonant frequencies of multiple cracked bars and application for crack detection. *Nondestructive Testing and Evaluation*, 34(3), 299–323. https://doi.org/10.1080/10589759.2019.1605604

[22]. N.T. Khiem, N.M, Tuan, P.T.B. Lien (2021). Crack identification in beam by antiresonant frequencies. *Vietnam Journal of Mechanics*, 43 (4), 389–405. https://doi.org/10.15625/0866-7136/16710

[23]. N.T. Khiem, T. H. Tran (2014). A procedure for multiple crack identification in beam-like structures from natural vibration mode. *Journal of Vibration and Control*, 20(19), 1417–1427. https://doi.org/10.1177/1077546312470478